Combustion and Flame 161 (2014) 3073–3084

Contents lists available at ScienceDirect

Combustion and Flame

journal homepage: www.elsevier.com/locate/combustflame

Heat release rate markers for premixed combustion

Zacharias M. Nikolaou *, Nedunchezhian Swaminathan

Cambridge University, Department of Engineering, Trumpington Street, Cambridge CB2 1PZ, UK

ARTICLE INFO

Article history:
Received 18 November 2013
Received in revised form 18 March 2014
Accepted 21 May 2014
Available online 16 June 2014

Keywords:
Heat release rate imaging
Premixed combustion
Flame markers
Laser diagnostics
Direct numerical simulation
Mild combustion

ABSTRACT

The validity of the commonly used flame marker for heat release rate (HRR) visualization, namely the rate of the reaction $OH + CH_2O \Leftrightarrow HCO + H_2O$ is re-examined. This is done both for methane–air and multi-component fuel–air mixtures for lean and stoichiometric conditions. Two different methods are used to identify HRR correlations, and it is found that HRR correlations vary strongly with stoichiometry. For the methane mixture there exist alternative HRR markers, while for the multi-component fuel flame the above correlation is found to be inadequate. Alternative markers for the HRR visualization are thus proposed and their performance under turbulent conditions is evaluated using DNS data.

1. Introduction

Heat release rate (HRR) is a very important quantity in the study of laminar and turbulent reacting flows. From a practical view point, the spatial distribution of heat release is useful to discern flames and their locations. This spatial distribution directly influences important physical processes such as flame–turbulence interaction, sound generation [1] and its interaction with flames resulting in combustion instabilities [2,3], determining the behaviour of practical devices such as industrial or aero gas turbines. Although a quantitative measurement of HRR is of great importance from both theoretical and practical view points, it is a challenging task as it involves accurate measurement of the order of 50 or more scalar concentrations and temperature simultaneously, since the local heat release rate is given by:

$$\dot{Q} = \sum_{\alpha=1}^{N} \dot{\omega}_\alpha h^0_{f,\alpha} \tag{1}$$

where $N \geqslant 50$ is the number of species involved in the oxidation of the fuel species, $h^0_{f,\alpha}$ is the standard enthalpy of formation for species α and $\dot{\omega}_\alpha$ is its reaction rate. A quantitative measurement of HRR is a daunting task at this time and has been attempted rarely. However, useful correlations for qualitative estimates of local HRR have been proposed in past studies [4–6]. The primary aims of those studies [4–6], were to identify a scalar having good, possibly linear correlation with the local heat release rate. It was observed by Najm and his co-workers [4–6] that the formyl radical, HCO, showed a good correlation with the local heat release rate for stoichiometric and slightly rich (equivalence ratio, ϕ, of 1.2) methane and dimethylether–air laminar flames. This correlation was also found to be insensitive to flame stretch (strain and curvature) effects resulting from flame–vortex interaction. As Eq. (1) suggests, the chemical kinetics model used in the computations of laminar flames would also impart due influences on this correlation. Thus, two chemical mechanisms, one involving 46 reactions and 16 species [7], and GRI Mech 1.2 involving 177 reactions and 32 species, were tested and it was concluded that the correlation of HCO with local HRR was not disturbed. This reasonably robust correlation, at least for the conditions tested in [4–6] was attributed to the following two reasons: (1) HCO is a major intermediate species in the oxidation of CH_4 to CO_2 and (2) the production of HCO from formaldehyde, CH_2O, is directly dependent on the rate of the reaction $O + CH_3 \Leftrightarrow H + CH_2O$, which was found to have the largest fractional contribution to the local HRR. The production of HCO from CH_2O occurs through $OH + CH_2O \Leftrightarrow HCO + H_2O$ and $H + CH_2O \Leftrightarrow HCO + H_2$. Since the formyl radical is produced in these elementary reactions and the signal to noise ratio for laser induced fluorescence of HCO is generally low compared to OH and CH_2O, the product of OH and CH_2O signals was proposed to be an indicator for the HRR. However, a recent study [8] showed that these correlations involving the formyl radical and, the formaldehyde and hydroxyl radicals, are inadequate for fuel rich mixtures of unsaturated hydrocarbons and for oxygenated fuels. Also, it was suggested [8] that the

* Corresponding author.
E-mail addresses: zn209@cam.ac.uk (Z.M. Nikolaou), ns341@cam.ac.uk (N. Swaminathan).

http://dx.doi.org/10.1016/j.combustflame.2014.05.019
0010-2180/

formaldehyde-based correlation is adequate when the major chemical path for fuel oxidation involves the methyl, CH_3 radical, and correlations involving ketyle, HCCO radicals, become more appropriate if the major oxidation route bypasses the methyl radical. Of course, it is imperative that a validation step for these correlations would be required if the flame conditions change from those investigated in the above studies. It is also worth to note that the formaldehyde-based correlation, i.e. [OH][CH_2O], where [A] indicates the molar concentration of species A, has been used in a number of studies, for example [9–17], as the de facto standard to infer heat release rate related information in laminar and turbulent premixed flames irrespective of the fuel mixture composition and stoichiometry.

The prime objective of this study is to assess the formaldehyde-based correlation and propose new correlations, if required, for a syngas containing multiple fuel species and other species, specifically CO, H_2, CH_4, H_2O and CO_2 in a proportion akin to Blast Furnace Gas (BFG). Although this gas has low calorific value, its use for power generation is of interest to gas turbine industries [18]. The formaldehyde-based correlation is also revisited for laminar methane–air flames. The specific aim of this study is to assess the HRR correlations based on formaldehyde and those proposed in the present study for turbulent premixed flames using direct numerical simulation (DNS) data. This kind of rigorous assessment for turbulent flames is uncommon and the past assessments are predominantly for one or two-dimensional laminar flames.

The outline of this paper is as follows. Since details of the DNS data used in this study have been reported in [19,20], brief details relevant for this study are given in Section 2 along with the conditions for the unstrained laminar flames. The fractional influence and error criteria used in this study to assess the local correlation between chemical markers and the HRR are explained in Section 3. The results are discussed in Section 4 and the conclusions are summarized in the final section.

2. DNS databases

The DNS databases involve freely propagating flames of undiluted methane–air mixture [20], diluted methane–air mixture [20], both having an equivalence ratio, ϕ, of 0.8, and an undiluted multi-component fuel–air mixture [19] with $\phi = 1.0$. The multi-component fuel mixture is at 800 K and 1 atm. It is composed of CO, H_2, H_2O, CO_2 and CH_4 and the mole fraction percentages of these species are given in Table 1. This composition is typical of a BFG mixture [18], or a low hydrogen content syngas mixture [21–23]. At these conditions the laminar flame speed is $s_l = 2.5\ \mathrm{ms}^{-1}$ and the flame thickness $\delta_l = 0.75$ mm, where $\delta_l = (T_p - T_r)/\max(dT/dx), T_r$ is the reactant temperature and T_p is the product temperature. The methane fuel mixture is at 600 K and 1 atm. At this conditions $s_l = 1.18\ \mathrm{ms}^{-1}$ and $\delta_l = 0.37$ mm. Further details of the mild case mixture can be found in [20]. Table 2 gives the turbulence parameters for the DNS databases. u_{rms} is the rms value of fluctuating velocity, with an integral length scale l_{int} on the reactant side. The turbulence Reynolds number is $\mathrm{Re} = u_{rms} \cdot l_{int}/\nu_r$, the Damkohler number is $\mathrm{Da} = (l_{int}/u_{rms})/(\delta/s_l)$ and the Karlovitz number is $\mathrm{Ka} = (\delta/\eta_k)^2$. The Zeldovich thickness is defined as $\delta = \nu_r/s_l$, where ν_r is the kinematic viscosity on the reactant side, and $\bar{u}_{in}$ is the mean inlet velocity.

Table 2
Turbulence parameters for the DNS.

Case	u_{rms}/s_l	l_{int}/δ	Re	Da	Ka	$\bar{u}_{\mathrm{in}}/s_l$
A	3.18	16.54	52.66	5.19	1.39	2.6
B	14.04	16.43	230.69	1.17	12.97	4.8
C	2.19	17.65	38.5	5.64	0.92	3.0
D	9.88	6.8	96.1	0.69	11.9	15.1

The computational domain size and resolution parameters for cases C and D can be found in [20]. For case A the domain length in the x, y and z directions is $L_x = 14$ mm, and $L_y = L_z = 7$ mm respectively. The resolution for case A is $N_x = 768$, $N_y = N_z = 384$ ensuring that there are at least 20 grid-points in the minimum reaction zone thickness of all species present. For case B $L_x = 21$ mm, and $L_y = L_z = 7$ mm with the corresponding number of grid-points is $N_x = 1632$, $N_y = N_z = 544$. The resolution is dictated by the turbulence scale in case B, giving $\delta_r = 2.5\eta_k$, where δ_r is the diagonal distance in a computational unit cell.

3. Analysis

The objective is to find suitable flame markers which correlate with the HRR preferably as much linearly as possible. In that respect a series of laminar unstrained premixed flame computations have been performed using the PREMIX code of the CHEMKIN package [24,25], at $p = 1$ atm and $T_r = 800$ K. The computations have been performed both for methane–air and multi-component fuel–air mixtures (to match the DNS), and a mixture-averaged formulation was used for the species diffusivities. GRI Mech 3.0 [26] is used in the computations since it is a well validated mechanism for methane combustion which is one of the fuels of interest. Furthermore, the skeletal mechanism derived in [27] from GRI Mech 3.0, was shown to perform reasonably against experimental flame speed and ignition delay data for multi-component fuel mixtures, thus justifying the use of GRI Mech 3.0 in this study.

The first method of the analysis is to rank elementary reactions based on their fractional contribution to the total HRR, and then to investigate whether the highest ranking reactions show good correlations with the heat release rate. The second method is based on an error estimator function which can be used to directly evaluate the spatial correlation of the heat release rate with a scalar of our choice. These two methods are described below.

3.1. Fractional influence method

This method is based on identifying a reaction imparting the most fractional influence on the overall HRR. The heat released by a reaction $r, \dot{q}_r$, across the flame brush of an unstrained premixed flame is given by:

$$\dot{q}_r = \int_x \dot{w}_r(x) \sum_\alpha h^0_{f,\alpha}(\nu''_{r,\alpha} - \nu'_{r,\alpha}) dx \tag{2}$$

Table 1
Fuel mixture composition in molar percentages used for the DNS. Note that the oxidiser for cases A, B and C is atmospheric air, while the oxidiser for case D (corresponding to Case B in [20]) is air diluted with combustion products.

Case	T_r (K)	ϕ	p (atm)	CO	H_2	H_2O	CO_2	CH_4
A, B	800.0	1.0	1.0	62.687	1.88	16.000	18.806	0.627
C	600.0	0.8	1.0	0.0	0.0	0.0	0.0	100.0
D (diluted)	1500.0	0.8	–	–	–	–	–	100.0

where $\dot{w}_r$ is the net reaction rate of reaction r, $h^0_{f,\alpha}$ is the formation enthalpy of species α, and $\nu''_{r,\alpha}$ and $\nu'_{r,\alpha}$, are the stoichiometric coefficients of species α in reaction r in the products and reactants respectively. The standard state of 1 atm and 298.15 K is used for the calculation of the species formation enthalpies. Having calculated $\dot{q}_r$ each reaction is then ranked according to its fractional contribution on the total HRR, $f_{qr} = 100 \cdot |\dot{q}_r|/|\dot{Q}_t|$, where $\dot{Q}_t$ is the total HRR across the flame brush:

$$\dot{Q}_t = \sum_r \dot{q}_r \tag{3}$$

Thus, $\sum_r f_{qr} = 100$ and, positive and negative values of f_{qr} respectively denote endothermic and exothermic reactions. This fraction is not the same as those used in earlier studies of Najm and his co-workers [4–6] and in [8], where a particular location inside a flame was considered. Although both of these methods are equally good, the integral method gives an overall measure to identify a reaction having the largest fractional influence on the total integrated heat release rate. The reaction identified thus is then used to find chemical markers for the HRR and the performance of these markers for turbulent conditions is evaluated using the DNS data described briefly in Section 2.

3.2. Error estimator method

In this approach, an error measure $Z(v)$ for a variable v, which may be a reliable HRR marker is defined as:

$$Z(v) = \int_x \left(\frac{|\dot{Q}(x)|}{\max(|\dot{Q}(x)|)} - \frac{|v(x)|}{\max(|v(x)|)} \right)^2 dx \tag{4}$$

where v can be any variable of our choice such as the concentration of a species or the rate of a reaction. This error, Z, may then be ranked for every variable v using $Z^+ = 100 \cdot Z/\max(Z)$. It is clear that the function Z gives an estimate of the error associated with the variable v, normalized using its maximum value as in Eq. (4), and spatially matched normalized HRR. The choice of v is of course not unique, however for any given variable v the one which minimizes Z would imply the best correlation with the HRR. The mass density ρY_α of a species α, and the net rate of a reaction r, $\dot{w}_r$, are used for v to find good HRR markers associated with the concentration of a species and with the rate of a reaction respectively. In the case $v = \dot{w}_r$, this may not be an exact method since the rate of a reaction r may have both positive and negative parts thus contributing ambiguously to the error estimator Z. However, the top-correlating reactions when $v = \dot{w}_r$ were found to have either only positive or negative contributions across the flame brush, thus not influencing the above definition.

4. Results and discussion

4.1. Methane fuel–air mixtures

Figures 1(a) and 2(a) show f_{qr} for the methane–air mixtures having $\phi = 0.5$ and 1.0 respectively. Only the top 15 reactions are shown for convenience. For all conditions the major heat consuming reaction is the chain branching reaction $H + O_2 \Leftrightarrow O + OH$. For $\phi = 0.5$ the major heat releasing reactions are $OH + CO \Leftrightarrow H + CO_2$ followed by $O + CH_3 \Leftrightarrow H + CH_2O$. For $\phi = 1.0$ this balance is changed. It is important to note that the reaction $O + CH_3 \Leftrightarrow H + CH_2O$ was also found to have the largest fractional influence on the HRR in [4], and also in [8] who used a more detailed mechanism [28]. What is noteworthy is that the reaction $OH + CH_2O \Leftrightarrow HCO + H_2O$ does not contribute largely to the HRR for $\phi = 0.5$, and it does not even appear in the top 15 reactions for $\phi = 1.0$ as one can see from Fig. 2. Furthermore, the relatively small contribution of the reaction $OH + CH_2O \Leftrightarrow HCO + H_2O$ to the HRR was also observed in [8]. The variation of $|\dot{Q}|^+ = |\dot{Q}|/\max(|\dot{Q}|)$ with the normalized net rates $\dot{w}^+_r = \dot{w}_r/\max(\dot{w}_r)$, of the top three reactions is shown in Figs. 1(b) and 2(b). It is clear that a large fractional contribution of a reaction to the HRR does not automatically imply that this will have a good correlation with the HRR. For example the reaction $OH + CO \Leftrightarrow H + CO_2$ having the highest exothermic fractional influence for the $\phi = 0.5$ flame, shows a poorer correlation than the reaction $O + CH_3 \Leftrightarrow H + CH_2O$ which has the second largest exothermic fractional influence. Similar arguments apply for the stoichiometric case also, and thus this method does not help to identify HRR markers.

Consequently, we use the error measure $Z(\rho Y_k)$, defined in Eq. (4). The results are shown in Fig. 3 for the $\phi = 1$ case, where the error measure is normalized using $Z^+ = 100 \cdot Z/\max(Z)$ as noted earlier. Of all the species, the HCO concentration minimizes Z^+ suggesting that this species is expected to have the best possible correlation with the HRR. HCO was also found to give the best correlation for the $\phi = 0.5$ case (not shown). Indeed one observes this in the corresponding figure on the right. This result for [HCO] is consistent with previous studies [4–6]. One also observes from Fig. 3(b) that as Z^+ increases the linearity of the correlation with the HRR becomes poorer, and overall these results help justifying the use of Eq. (4) for systematically identifying heat release rate correlations.

As noted in the introduction, the signal to noise ratio for HCO in laser diagnostics is generally low, and thus alternative markers were proposed for the HRR. This proposition was based on the reactions which are thought to be responsible for the majority of HCO production [4–6], and one of these reactions is $OH + CH_2O \Leftrightarrow HCO + H_2O$. Thus measuring [OH][$CH_2O$] which is proportional to the rate of this reaction was expected to give an estimate of the HCO concentration and thus serve as a good marker for the heat release rate. In this study, this hypothesis is re-examined using $Z(\dot{w}_r)$. The results of this analysis are shown in Figs. 4 and 5. For the $\phi = 0.5$ case, the chain-terminating reaction $H + HO_2 \Leftrightarrow O_2 + H_2$ has the minimum error as per Eq. (4), followed by the chain-carrying reaction $H + HO_2 \Leftrightarrow O + H_2O$. Both of these reactions are exothermic and despite the fact that they do not contribute much to the overall HRR (see Fig. 1) they have good spatial correlations with the heat release rate. Also shown in Fig. 4 for comparison, is the rate of $OH + CH_2O \Leftrightarrow HCO + H_2O$. This reaction has an overall larger error than the reactions $H + HO_2 \Leftrightarrow O_2 + H_2$ and $H + HO_2 \Leftrightarrow O + H_2O$. As one can see from Fig. 4 this error occurs for relatively low heat release rates where the correlation of this reaction is observed to be poorer relative to $H + HO_2 \Leftrightarrow O_2 + H_2$ and $H + HO_2 \Leftrightarrow O + H_2O$. For large heat release rates the correlation of $OH + CH_2O \Leftrightarrow HCO + H_2O$ is observed to be better than either $H + HO_2 = O_2 + H_2$ and $H + HO_2 \Leftrightarrow O + H_2O$, however since $Z(\dot{w}_r)$ gives a measure of the spatial correlation across the whole of the flame brush this is smallest for $H + HO_2 \Leftrightarrow O_2 + H_2$ and $H + HO_2 \Leftrightarrow O + H_2O$ implying an overall better correlation with the HRR. Furthermore, the rate of the reaction $OH + CH_2O \Leftrightarrow HCO + H_2O$ shows a non-zero HRR for zero reaction rate, as one can see from Fig. 4 which is consistent with previous studies [4–6,8]. Thus the correlation based on this reaction cannot be used to identify local extinction. $H + HO_2 \Leftrightarrow O_2 + H_2$ and $H + HO_2 \Leftrightarrow O + H_2O$ on the other hand show zero HRR at zero rates, implying that these markers can capture local extinction as well if they can be identified using laser diagnostics. For the $\phi = 1.0$ case, the values of Z^+ are altered significantly, with the endothermic reactions $O + CH_3OH \Leftrightarrow OH + CH_3O$ and $O + CH_4 \Leftrightarrow OH + CH_3$ having the smallest errors thus implying the best correlations with the HRR.

Therefore it is clear that HRR correlation is strongly dependent on the equivalence ratio. In the hope to find a reasonable correlation across ϕ, the ϕ-averaged error $\bar{Z} = \sum_\phi Z/N_\phi$ where N_ϕ is the

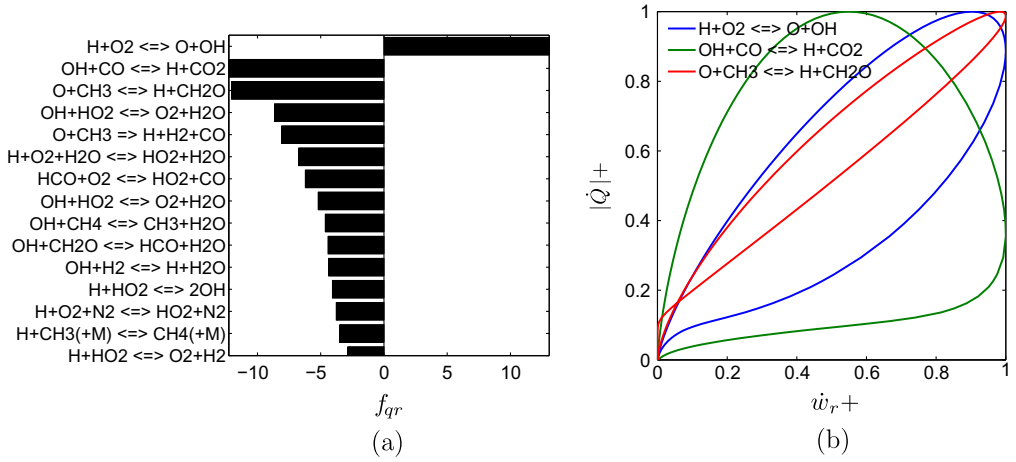

Fig. 1. Methane–air mixture with $\phi = 0.5$, $T_r = 800$ K and $p = 1$ atm.

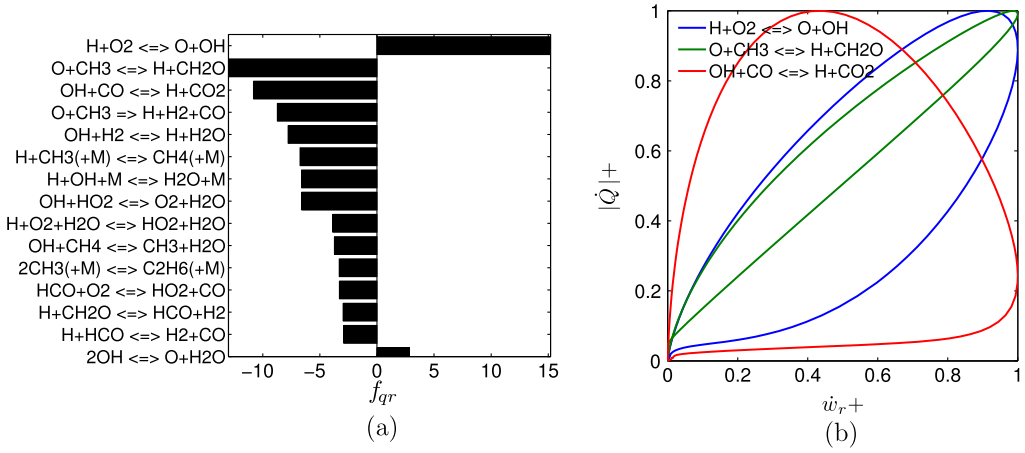

Fig. 2. Methane–air mixture with $\phi = 1$, $T_r = 800$ K and $p = 1$ atm.

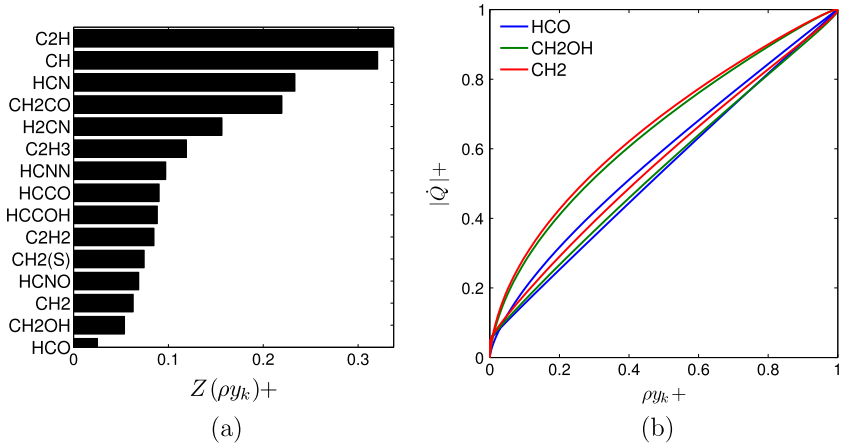

Fig. 3. Methane–air mixture with $\phi = 1$, $T_r = 800$ K and $p = 1$ atm.

total number of ϕ samples considered, can be used to extract the reaction with the best overall correlation across different stoichiometry. Towards this goal, and with lean combustion in mind, computations of laminar premixed flames for $0.5 \leqslant \phi \leqslant 1.0$ in steps of 0.1 have been conducted and $\overline{Z}$ calculated for all reactions. In a similar manner to the analysis using Z, the reactions are ranked based on the value of $\overline{Z}$. The results are shown in Fig. 6, using the GRI Mech 3 [26] and the San Diego [29] mechanisms. As noted in the introduction, the observed correlations depend on the chemical mechanism used. The use of the San Diego mechanism will help to elucidate this dependence and to see whether the same reactions showing the smallest $\overline{Z}$ for GRI Mech 3.0, also show the same trend for a different mechanism. Reactions ranking high in both mechanisms would thus imply possibly good HRR correlations for that

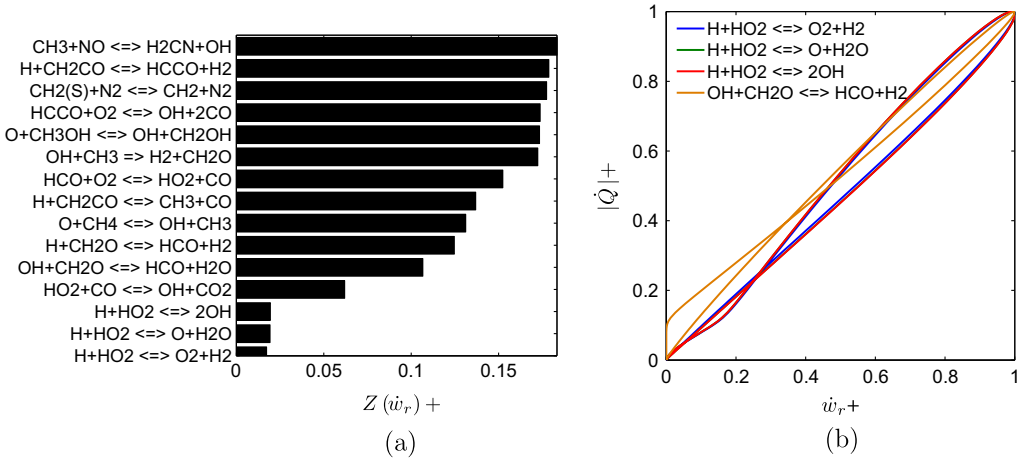

Fig. 4. Methane–air mixture with $\phi = 0.5$, $T_r = 800$ K and $p = 1$ atm.

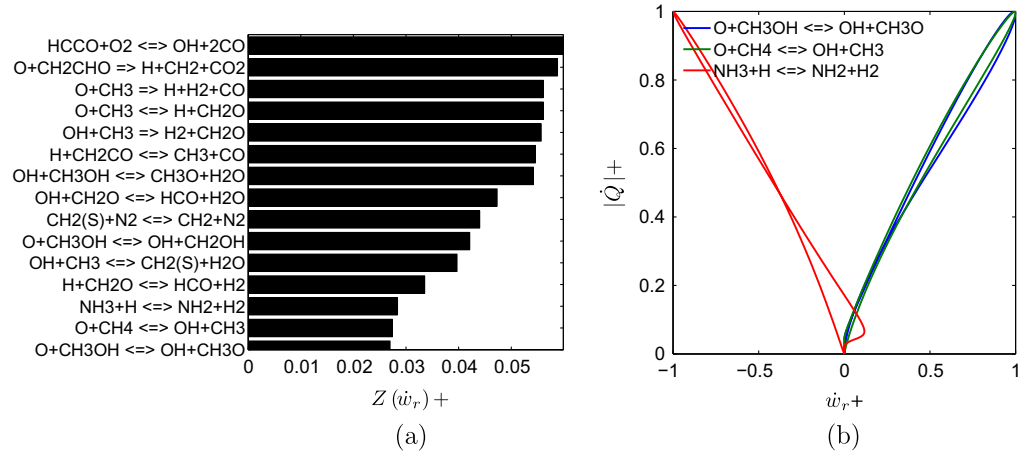

Fig. 5. Methane–air mixture with $\phi = 1$, $T_r = 800$ K and $p = 1$ atm.

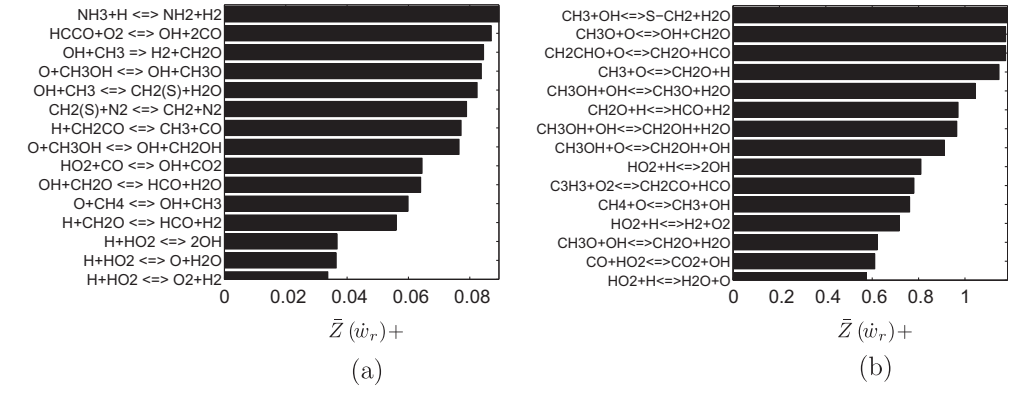

Fig. 6. ϕ-Averaged $Z(\dot{w}_r)$ for $0.5 \leqslant \phi \leqslant 1.0$ in steps of 0.1 equivalence ratio, using GRI Mech 3 (a) and San Diego (b) mechanisms.

particular reaction irrespective of the mechanism used. The results are shown in Fig. 6 on the right. Overall, $\overline{Z}$ is generally larger for the San Diego mechanism implying reduced spatial HRR correlations for the same reaction. However, the reaction $H + HO_2 \Leftrightarrow O_2 + H_2$ ranks 1st and 4th using the GRI and San Diego mechanisms respectively, while the reaction $H + HO_2 \Leftrightarrow O + H_2O$ ranks 2nd and 1st. The reaction $OH + CH_2O \Leftrightarrow HCO + H_2O$ commonly used for the HRR marker, ranks 6th for GRI Mech 3 and it does not even appear in the top 15 reactions for the San Diego mechanism. The reactions $O + CH_4 \Leftrightarrow OH + CH_3$ and $H + CH_2O \Leftrightarrow HCO + H_2$ are found to rank high for both mechanisms.

To shed some light into the performance of these markers for different equivalence ratios, one can study the $Z(\dot{w}_r)^+$ variation with ϕ. This variation is shown in Fig. 7 for the top six reactions appearing in Fig. 6, using GRI Mech 3.0 which shows the smaller Z. For lean mixtures, the reactions $H + HO_2 \Leftrightarrow O_2 + H_2$ and $H + HO_2 \Leftrightarrow O + H_2O$ have the smallest errors and thus the best correlations with the HRR. The reaction $H + HO_2 \Leftrightarrow 2OH$ shows almost the same

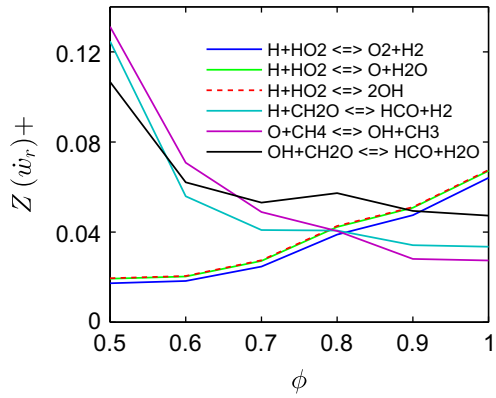

Fig. 7. $Z(\dot{w}_r)^+$ variation with ϕ for the top six reactions in GRI Mech 3 shown in Fig. 6.

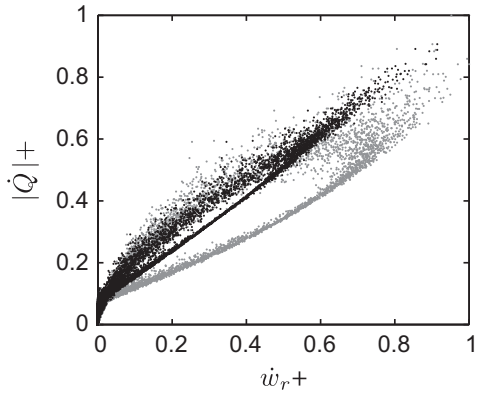

Fig. 8. Scatter plot of normalized heat release rate with $\dot{w}_r^+$ for OH + $CH_2O \Leftrightarrow$ HCO + H_2O (grey dots) and H + $CH_2O \Leftrightarrow$ HCO + H_2 (black dots) for case C in Table 1.

variation in error as the reaction H + $HO_2 \Leftrightarrow$ O + H_2O. The reaction OH + $CH_2O \Leftrightarrow$ HCO + H_2O has a much larger error than either of the above two reactions, implying a reduced correlation. As stoichiometry is approached, the error associated with the reaction OH + $CH_2O \Leftrightarrow$ HCO + H_2O decreases, and for $0.8 \leqslant \phi \leqslant 1.0$ becomes smaller than the error associated with the above two reactions implying a better HRR correlation. However, at the same time the errors associated with the reactions O + $CH_4 \Leftrightarrow$ OH + CH_3 and H + $CH_2O \Leftrightarrow$ HCO + H_2 also decrease and become less than the error for OH + $CH_2O \Leftrightarrow$ HCO + H_2O when $\phi \geqslant 0.7$. Thus, these results suggest that for very lean mixtures the rate of the reactions H + $HO_2 \Leftrightarrow O_2 + H_2$ or H + $HO_2 \Leftrightarrow$ O + H_2O, would serve as an unambiguous and good HRR marker, while for near-stoichiometric mixtures the rate of the reactions O + $CH_4 \Leftrightarrow$ OH + CH_3 or H + $CH_2O \Leftrightarrow$ HCO + H_2 seem a better choice. It is important to note at this point that the reaction OH + $CH_2O \Leftrightarrow$ HCO + H_2O was found not to be the primary source of formyl radicals in [8], which explains the increased error associated with this reaction observed in the current study. Instead, the reaction H + $CH_2O \Leftrightarrow$ HCO + H_2 was found [8] to be the major HCO formation path, which explains the relatively lower error associated with this reaction, since as already mentioned HCO correlates strongly with the HRR.

As already mentioned in the introduction, the derivation of HRR markers in past studies [4–6,8] was primarily based on laminar flame computations. Thus the effect of turbulence on the proposed correlations was not examined, and it is important to note that reactions showing high correlations for the laminar flames may not necessarily show high correlations for the turbulent case also, due to the effects of curvature and strain rate induced by turbulence. It is well known that these effects can impart different levels of influence on different species because of the difference in their molecular diffusivities and Lewis numbers. For example the curvature can strongly affect the spatial variation of lighter species such as atomic hydrogen. Thus, the proposed correlations of this study are tested for turbulent flames using the DNS data described in Section 2. Figure 8 shows a scatter plot of the HRR against the forward rates of reactions OH + $CH_2O \Leftrightarrow$ HCO + H_2O and H + $CH_2O \Leftrightarrow$ HCO + H_2, for case C in Table 1. The reactions O + $CH_4 \Leftrightarrow$ OH + CH_3 and H + $HO_2 \Leftrightarrow$ O + H_2O do not take place in the mechanism used for the DNS [31], hence these relationships cannot be tested. All quantities are normalized with respect to their instantaneous maximum values, and consistent with the results shown in Fig. 7, the reaction H + $CH_2O \Leftrightarrow$ HCO + H_2 shows a clearly improved correlation with the HRR compared to the reaction OH + $CH_2O \Leftrightarrow$ HCO + H_2O. In particular, the scatter is reduced significantly, and the linearity of the correlation is also improved. The results in Fig. 7 also show the reactions H + $HO_2 \Leftrightarrow O_2 + H_2$ and H + $HO_2 \Leftrightarrow$ 2OH to have smaller errors than the commonly used marker. Figure 9 shows the HRR against the rate of H + $HO_2 \Leftrightarrow O_2 + H_2$. Consistent with the results in Fig. 4, this reaction correlates better with the HRR in regions of low to intermediate HRR. At zero reaction rate, the HRR is observed to be zero as well, suggesting that this reaction may capture local extinction. Similar results were also observed to hold for H + $HO_2 \Leftrightarrow$ 2OH. For intermediate to high HRR however, the commonly used marker seems to perform better. In order to examine the influence of the chemical mechanism used in the DNS on the proposed HRR correlations, Fig. 10 shows the correlations of some of the top-correlating reactions using both GRI Mech. 3.0 [26] and Smooke's mechanism as used in the DNS [31], for the stoichiometric case. It is clear that there is a large difference on the HRR correlation for the reaction H + $HO_2 \Leftrightarrow O_2 + H_2$, similar to the one observed with the DNS data. This suggests that the poor correlation observed in the DNS data for relatively large values of the HRR is due to the chemical mechanism used (Smooke's mechanism) and not because of the correlation itself. Another important point is that the correlations of the other two reactions are relatively insensitive to the chemical mechanism used. This implies that the good correlation observed for H + $CH_2O \Leftrightarrow$ HCO + H_2 is not biased in any way when using Smooke's mechanism.

The performance of the marker H + $CH_2O \Leftrightarrow$ HCO + H_2 is also evaluated using a mild combustion DNS database. This database, corresponding to case B in [20], involves a methane–air mixture diluted with combustion products, at a turbulence level of $u_{rms}/s_l = 9.88$. The results are shown in Fig. 11. Both the commonly used marker and H + $CH_2O \Leftrightarrow$ HCO + H_2 show a significant scatter across all HRR values, with the majority of the points however falling on an almost straight line for both cases. In agreement with the

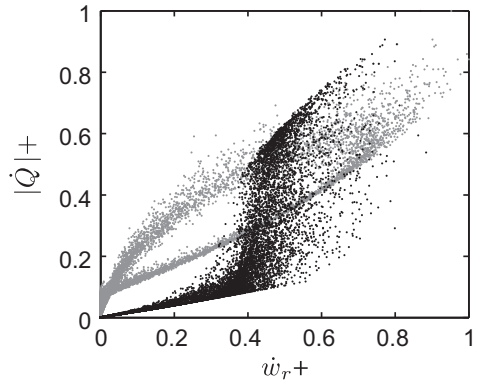

Fig. 9. Scatter plot of normalized heat release rate with $\dot{w}_r^+$ for OH + $CH_2O \Leftrightarrow$ HCO + H_2O (grey dots) and H + $HO_2 \Leftrightarrow O_2 + H_2$ (black dots) for case C in Table 1.

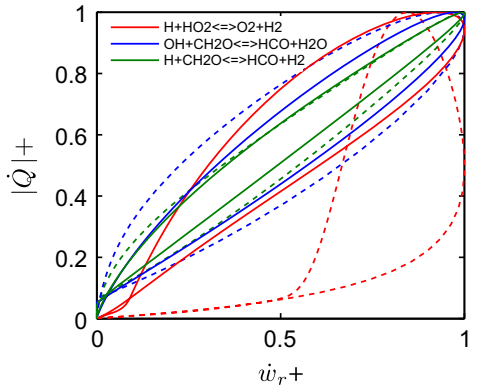

Fig. 10. A comparison of the top HRR-correlating reactions using GRI Mech 3.0 [26] (continuous lines) and Smooke [31] (dashed lines) mechanisms. The results are for a stoichiometric methane–air laminar flame.

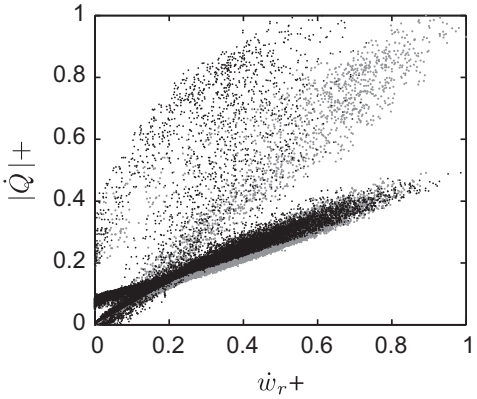

Fig. 11. Scatter plot of normalized heat release rate with $\dot{w}_r^+$ for $OH + CH_2O \Leftrightarrow HCO + H_2O$ (grey dots) and $H + CH_2O \Leftrightarrow HCO + H_2$ (black dots) for case D in Table 1.

results in Fig. 8, $H + CH_2O \Leftrightarrow HCO + H_2$ seems to be showing a relatively lower scatter suggesting that it may be a more reliable HRR marker, despite the chemical complexity of this fuel.

4.2. Multi-component fuel–air mixtures

In this section a similar analysis is carried out for a multi-component fuel mixture, as noted earlier. This fuel consists of CO, H_2, H_2O, CO_2 and CH_4 in the proportions given in Table 1. Figures 12 and 13 show f_{qr} for ϕ = 0.5 and 1.0 respectively, obtained using GRI Mech 3.0. For both equivalence ratios the reaction $OH + CO \Leftrightarrow H + CO_2$ has the highest fractional influence followed by the recombination reaction $H + O_2 + H_2O \Leftrightarrow HO_2 + H_2O$. However, for both conditions the recombination reaction appears to have the best correlation with the HRR as one can see from the corresponding figures on the right, despite the fact that it contributes only about 10% to the total HRR, whereas the reaction $OH + CO \Leftrightarrow H + CO_2$ contributes in both cases by more than 30%. The results obtained using the error-estimator analysis are shown in Fig. 14 for ϕ = 1.0, for the mass densities of various species. The error was found to be minimum for the concentration of HCO only for the stoichiometric mixture. However, this minimum error is observed to be significantly larger than the corresponding error for the stoichiometric methane–air mixture shown in Fig. 3. The influence of this increased error is reflected in the relatively poorer correlation with the HRR shown in Fig. 14(b). Thus, these results suggest that more than one species may be required for a good HRR correlation for the multi-component fuel–air mixture, although the carbon oxidation is expected to be through the methyl radical for this fuel mixture.

Figures 15 and 16 show $Z(\dot{w}_r)$ for $\phi = 0.5$ and 1.0 respectively. For lean mixtures the reaction $H + O_2 + H_2O \Leftrightarrow HO_2 + H_2O$ gives the smallest error and the best HRR correlation among the top three reactions identified. At stoichiometric conditions this reaction is trumped by the reaction $H + O_2 + M \Leftrightarrow HO_2 + M$. It is important to note here that despite the fact that both of the above two reactions are third-body recombination reactions they appear separately in the GRI Mech 3.0 dataset since the third body efficiency for H_2O in $H + O_2 + M \Leftrightarrow HO_2 + M$ is zero (see Eq. (6)). For both equivalence ratios considered, the commonly used marker i.e. the rate of the reaction $OH + CH_2O \Leftrightarrow HCO + H_2O$ does not appear in the top 15 reactions. This was also observed in [19] where this commonly used correlation was tested.

Following a similar analysis as in the previous section, Fig. 17 shows $\overline{Z}$ averaged across $0.5 \leqslant \phi \leqslant 1.0$ in steps of 0.1. This is done using both GRI Mech 3.0 [26] and Li et al. [30] mechanisms. The third body recombination reaction $H + O_2 + M \Leftrightarrow HO_2 + M$ is found to rank 1st and 3rd using the GRI and Li et al. mechanisms respectively, while the reaction $O + HO_2 \Leftrightarrow OH + O_2$ ranks 3rd and 1st respectively, indicating that these reactions are strong candidates to mark HRR. Overall though one may observe from Fig. 17, that the errors using the Li et al. mechanism are generally higher than using GRI Mech 3.0, implying that the correlation for the same reaction is generally weaker. Thus, in order to examine the error

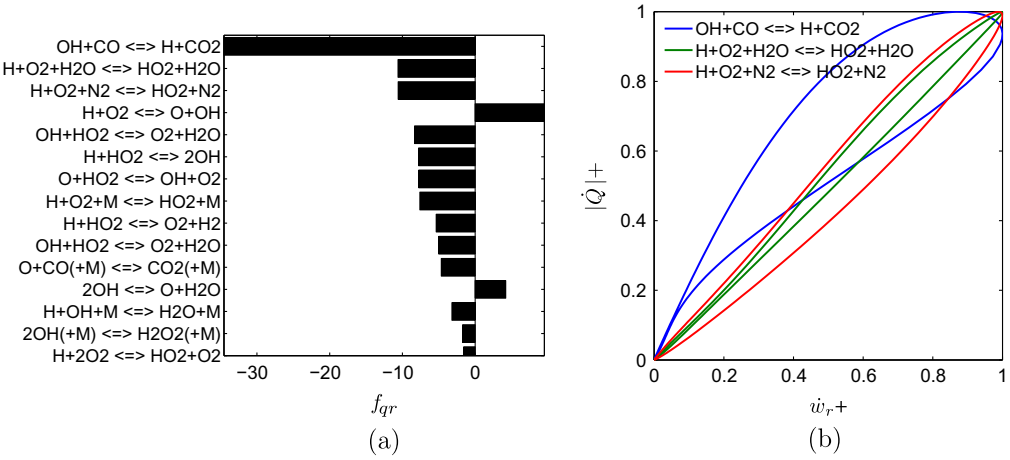

Fig. 12. Multi-component fuel–air mixture with $\phi = 0.5, T_r = 800$ K and $p = 1$ atm.

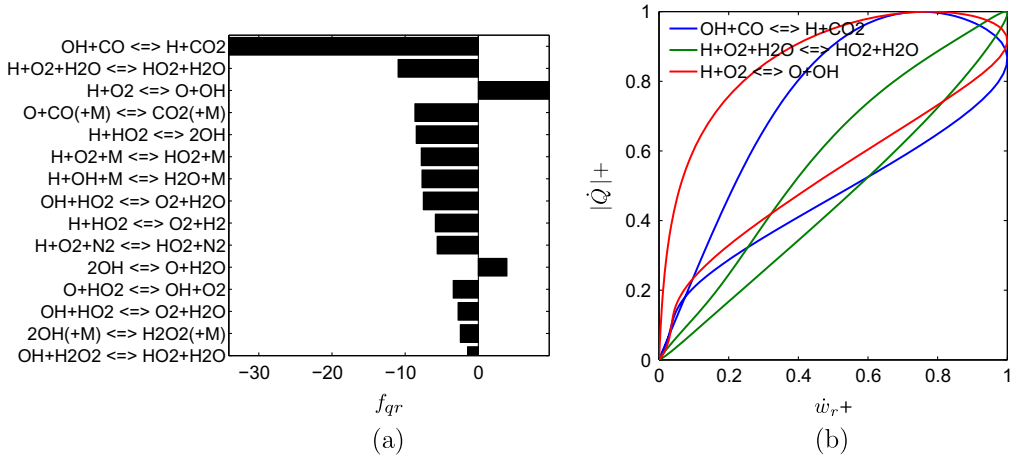

Fig. 13. Multi-component fuel–air mixture with $\phi = 1.0, T_r = 800$ K and $p = 1$ atm.

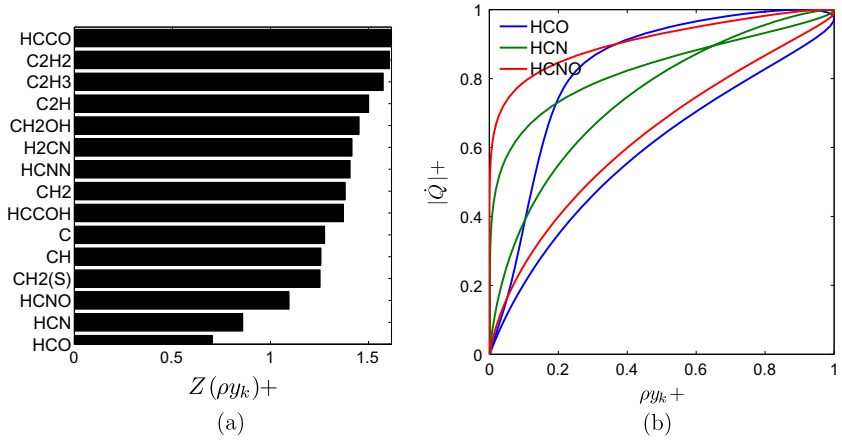

Fig. 14. Multi-component fuel–air mixture with $\phi = 1.0, T_r = 800$ K and $p = 1$ atm.

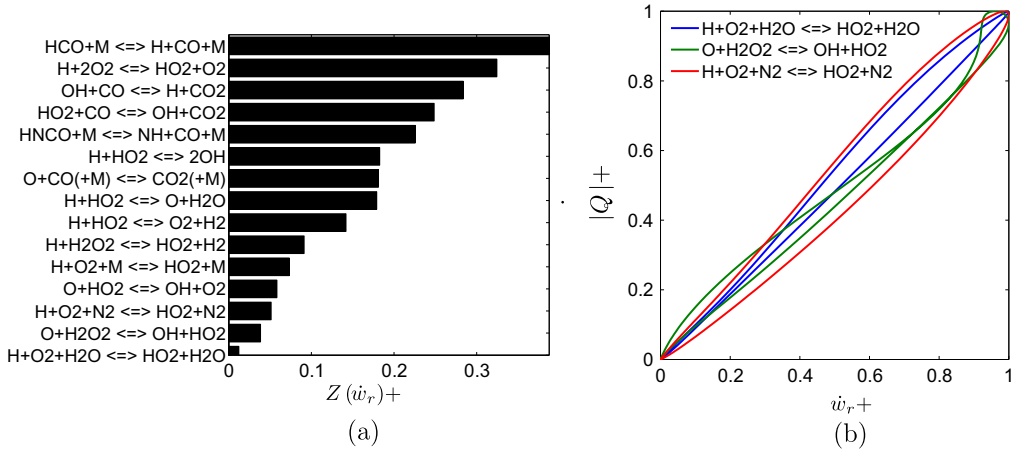

Fig. 15. Multi-component fuel–air mixture with $\phi = 0.5, T_r = 800$ K and $p = 1$ atm.

variation with the equivalence ratio, the top three reactions of Fig. 17 using GRI Mech 3.0 are considered. The results are shown in Fig. 18. The reaction $O + HO_2 \Leftrightarrow OH + O_2$ has larger errors compared with the other two reactions. The recombination reaction $H + O_2 + H_2O \Leftrightarrow HO_2 + H_2O$ has a smaller error than the reaction $H + O_2 + M \Leftrightarrow HO_2 + M$ at lean conditions. This behaviour changes at $\phi \simeq 0.7$ indicating that for near-stoichiometric conditions the rate of the reaction $H + O_2 + M \Leftrightarrow HO_2 + M$ is a better marker for the HRR.

The reverse rate of $H + O_2 + M \Leftrightarrow HO_2 + M$ is found to be negligible in comparison with the forward rate of this reaction, and thus the net rate is given by:

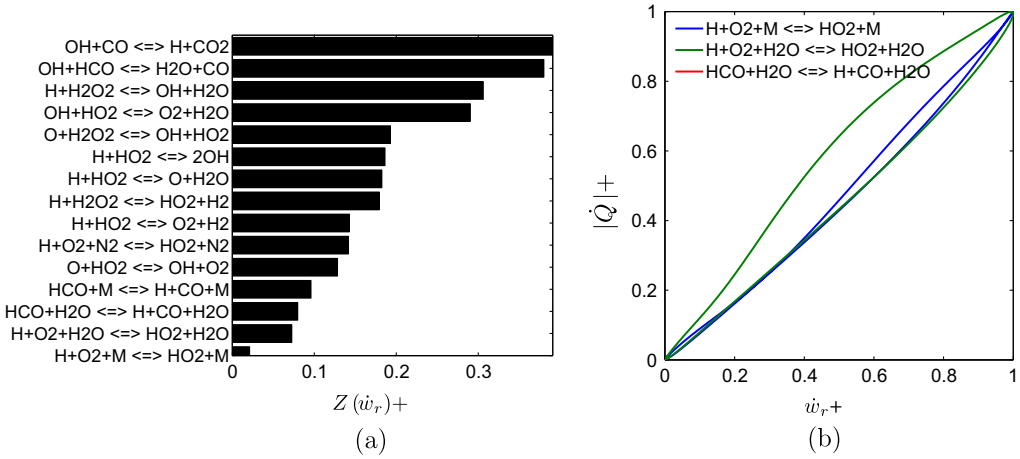

Fig. 16. Multi-component fuel–air mixture with $\phi = 1.0, T_r = 800$ K and $p = 1$ atm.

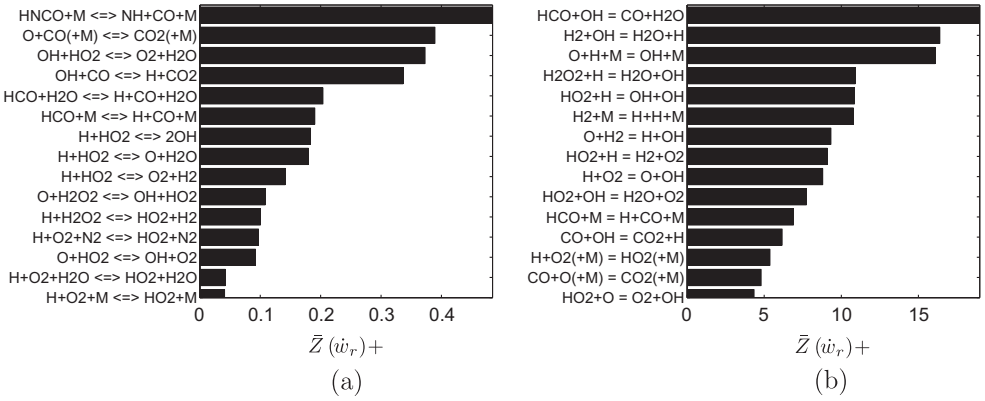

Fig. 17. ϕ-Averaged $Z(\dot{w}_r)$ for $0.5 \leqslant \phi \leqslant 1.0$ in steps of 0.1 equivalence ratio using GRI Mech 3 (a) and Li et al. (b) mechanisms.

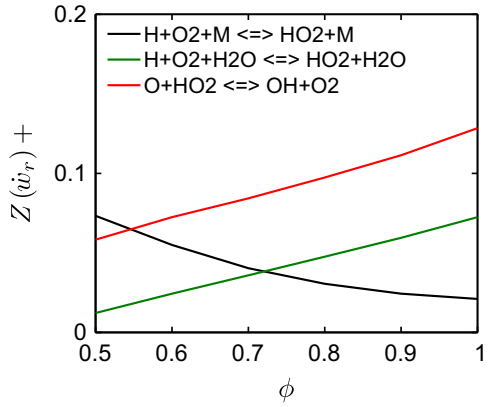

Fig. 18. $Z(\dot{w}_r)^+$ variation with ϕ for the top three reactions in GRI Mech 3 shown in Fig. 17.

$$\dot{w}_r \simeq k_f[\mathrm{H}][\mathrm{O}_2]\sum_{\alpha}\eta_{\alpha}[c_{\alpha}] \tag{5}$$

where η_α is the third body efficiency of species α, and k_f is the forward rate of this reaction. Eq. (5) suggests that the experimental estimation of this rate requires in addition to [H] and [O_2], the concentrations of all species which have non-zero third body coefficients. This is of course impossible since there are O(50) species present with non-zero third body coefficients. This issue can be alleviated by noting, as Eq. (4) suggests, that we are not in fact interested in the quantitative measurement of the rate of this reaction. We are rather interested in capturing a reasonably correct variation of the rate of this reaction across the flame brush, and how this correlates with the HRR as per Eq. (4). Rigorous analysis employing different species involved in the list of third body species for this reaction, revealed CO and CO_2 to primarily influence this variation. Thus, considering the third body efficiencies of these species only, taken from GRI Mech 3.0, one can estimate this variation using:

$$\dot{w} \sim T^{-0.86}[\mathrm{H}][\mathrm{O}_2](0.75[\mathrm{CO}] + 1.5[\mathrm{CO}_2]) \tag{6}$$

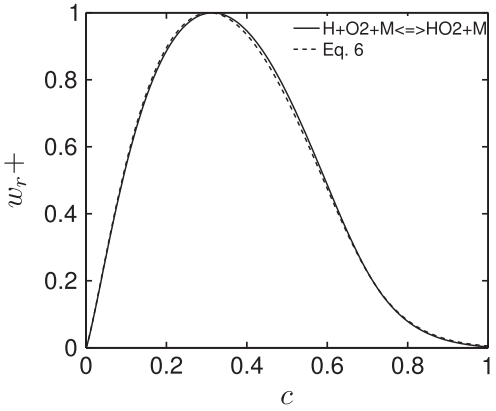

Fig. 19. Variation of normalized rate of H + O_2 + M ⇔ HO_2 + M and Eq. (6) across the flame.

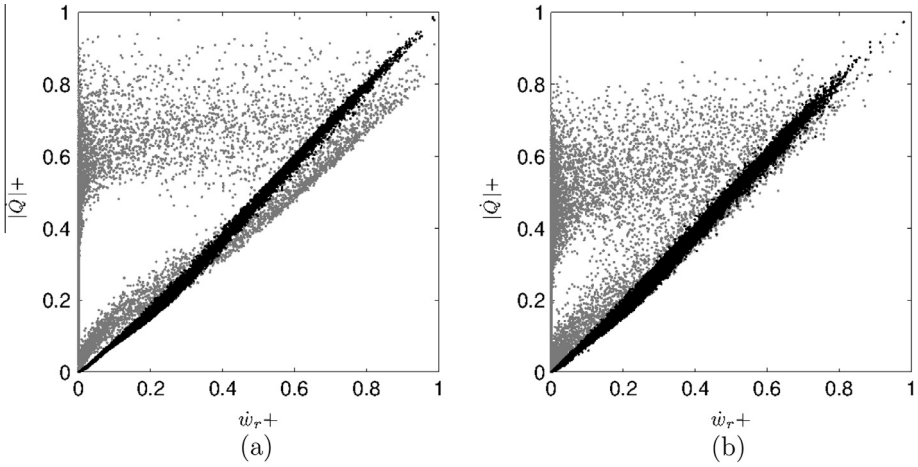

Fig. 20. Scatter plot of normalized heat release rate with normalized rate of OH + $CH_2O \Leftrightarrow$ HCO + H_2O (grey dots) and using Eq. (6) (black dots). The results are shown for for case A (a) and case B (b) in Table 1.

Figure 19 shows the net rate of H + O_2 + M $\Leftrightarrow$ HO_2 + M and that using Eq. (6) normalized with respect to their corresponding maximum values. It is clear that Eq. (6) captures the variation of this rate across the flame brush very well, and as a result Eq. (6) is expected to show the same (good) correlation with the HRR. To validate these results, Fig. 20 shows scatter plots of the normalized HRR against the normalized rate of OH + $CH_2O \Leftrightarrow$ HCO + H_2O and Eq. (6). The commonly used flame marker shows a poor correlation with the HRR, and it was shown in [19] that this is not a result of the turbulence–scalar interaction. The flame marker calculated from Eq. (6) on the other hand, shows an almost linear correlation with the HRR with minimal scatter, for both turbulence levels considered.

Figure 21 shows the normalized HRR against the rate of OH + $CH_2O \Leftrightarrow$ HCO + H_2O, and of O + $HO_2 \Leftrightarrow$ OH + O_2 which is found to rank high in Fig. 17. Although this reaction shows a larger error in comparison with H + O_2 + M $\Leftrightarrow$ HO_2 + M, it has no temperature dependence in both the GRI Mech 3.0 and Li et al. datasets, and may thus be easier for laser diagnostics, but one needs to image O and HO_2. Consistent with the previous analysis which revealed the rate of O + $HO_2 \Leftrightarrow$ OH + O_2 to have a larger error, it shows a poorer correlation with the HRR in comparison to the rate of the third body reaction. However, as one can see from Fig. 21, O + $HO_2 \Leftrightarrow$ OH + O_2 also gives an improved correlation with the HRR compared to the commonly used flame markers.

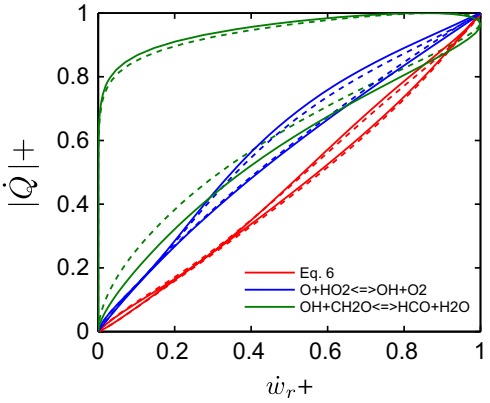

Fig. 22. A comparison of the top HRR-correlating reactions using GRI Mech 3.0 [26] (continuous lines) and Nikolaou et al. [27] (dashed lines) mechanisms.

Furthermore, the results shown in Fig. 17 suggest that these proposed correlations will be improved for leaner mixtures, which are of practical interest. The validity of these correlations for mixtures with higher H_2 levels and in non-premixed combustion is a subject of future work.

Following a similar analysis like in Section 4.1 Fig. 22 shows the correlations of the proposed markers using both GRI Mech 3.0 [26]

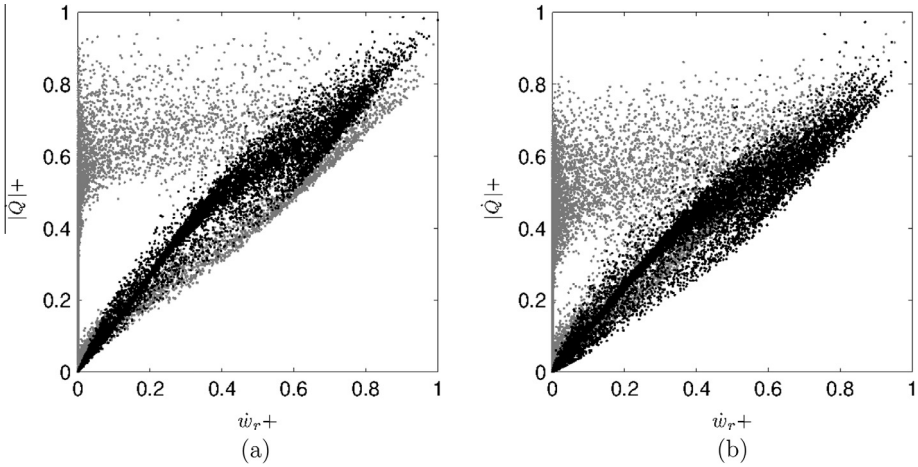

Fig. 21. Scatter plot of normalized heat release rate with normalized rates of OH + $CH_2O \Leftrightarrow$ HCO + H_2O (grey dots) and O + $HO_2 \Leftrightarrow$ OH + O_2 (black dots). The results are shown for for case A (a) and case B (b) in Table 1.

Table 3
The range of equivalence ratios where the respective reactions show improved correlations with the HRR (for the methane and diluted methane mixtures) as opposed to the commonly used marker, using GRI Mech 3.0 [26]. The San Diego [29] and Li et al. [30] mechanisms were also used to confirm these results (see Figs. 6 and 17). For the multi-component fuel two alternative correlations are proposed.

Fuel	ϕ	Reaction	Validation
CH_4	$\leqslant 0.9$	$H + HO_2 \Leftrightarrow O_2 + H_2$	Laminar
CH_4	$\leqslant 0.9$	$H + HO_2 \Leftrightarrow O + H_2O$	Laminar
CH_4	$\leqslant 0.9$	$H + HO_2 \Leftrightarrow 2OH$	Laminar
CH_4	0.6–1.0	$H + CH_2O \Leftrightarrow HCO + H_2$	DNS ($\phi = 0.8$) [20] + Laminar
Dilluted-CH_4	–	$H + CH_2O \Leftrightarrow HCO + H_2$	DNS ($\phi = 0.8$) [20]
CH_4	0.7–1.0	$O + CH_4 \Leftrightarrow OH + CH_3$	Laminar
Multi-component	$\geqslant 0.55$	$H + O_2 + M \Leftrightarrow HO_2 + M$, Eq. (6)	DNS ($\phi = 1.0$) [19] + Laminar
Multi-component	$\leqslant 0.55$	$O + HO_2 \Leftrightarrow OH + O_2$	DNS ($\phi = 1.0$) [19] + Laminar

and the skeletal mechanism of Nikolaou et al. [27]. It is clear that the correlations are relatively insensitive to the use of the skeletal mechanism. As a result, the skeletal mechanism does not in any way influence the good correlations observed with the DNS data in Figs. 20 and 21.

5. Proposed HRR markers

Table 3 shows a summary of all the previous analysis, essentially encapsulating the results shown in Figs. 6, 7, 17 and 18. Table 3 shows the range of equivalence ratios where each reaction has an improved correlation with the HRR as opposed to the commonly used marker. Also shown is the validation procedure (DNS, laminar) for the proposed correlations. It was shown in Section 4.1, that the chemical mechanism used in the methane DNS introduces a bias in the HRR correlation for the first three reactions. As a result, the DNS correlations for these reactions cannot be considered plausible. These reactions involving, H and HO_2, were however validated in the laminar case, and were shown to give improved correlations for $\phi <\simeq 0.9$ as per Fig. 6. For relatively lean to stoichiometric conditions, the reactions $H + CH_2O \Leftrightarrow HCO + H_2$ and $O + CH_4 \Leftrightarrow OH + CH_3$ also give improved correlations with the HRR. For the multi-component fuel flame the third body reaction $H + O_2 + M \Leftrightarrow HO_2 + M$ from which Eq. (6) was derived, is observed to give very good HRR correlations for relatively lean to stoichiometric mixtures. Although the reaction $O + HO_2 \Leftrightarrow OH + O_2$ has a slightly poorer correlation with the HRR, laminar flame computations suggest it to perform better for very lean conditions.

It is important to note at this point that despite the drawbacks associated with the $[OH][[CH_2O]$ correlation, it is widely used because it is easy to measure. Although the $[OH][[CH_2O]$ correlation does not provide quantitative equally good results, it can still be used to mark locations of increased chemical activity. The alternative correlations proposed in this study provide improved quantitative correlations but require the simultaneous measurement of more than one species, some of which may be difficult to measure. These markers should thus be taken as a guideline which will help in the future to develop the necessary techniques needed for the measurement of the associated species.

6. Conclusions

In this study, the validity of the rate of the reaction $OH + CH_2O \Leftrightarrow HCO + H_2O$ as a reliable heat release rate (HRR) marker is re-examined. This is done in the perspective of lean combustion of both methane–air mixtures and for multi-component fuel–air mixtures. Two different methods are used to identify HRR markers. In the first method, the fractional influence of all reactions to the total HRR across the flame brush is examined, and it is found that the top endothermic or exothermic reactions do not necessarily show the highest HRR correlations. In the second method, an error-estimator, $Z(v)$ is proposed, where v can be a scalar of our choice. The scalar minimizing Z is identified as the one having the best HRR correlation. This is tested using a number of quantities, and the well established HCO concentration is recovered as the best marker for the HRR of methane–air mixtures.

For both the methane–air and the multi-component fuel–air mixtures considered, the correlations identified in this study are found to depend on the equivalence ratio. It is shown that for the methane fuel–air mixture there exist reactions which correlate better with the HRR. For lean mixtures, the HRR is found to correlate stronger with the rates of the reactions $H + HO_2 \Leftrightarrow O_2 + H_2$ and $H + HO_2 \Leftrightarrow O + H_2O$ especially at low values of the heat release rate. The reaction $OH + CH_2O \Leftrightarrow HCO + H_2O$ on the other hand shows a better correlation at higher values of HRR rate. For near-stoichiometric mixtures, the HRR correlates better with the rates of the reactions $O + CH_4 \Leftrightarrow OH + CH_3$ and $H + CH_2O \Leftrightarrow HCO + H_2$. The last correlation is tested under turbulent conditions using DNS data of a methane–air premixed flame, and mild combustion involving a methane–air mixture diluted with combustion products, and it is observed that the correlation based on H and CH_2O with the HRR is more linear and has reduced scatter compared to that based on OH and CH_2O.

For the multi-component fuel–air mixture strong HRR correlations were observed primarily with third body recombination reactions. This correlation is also evaluated for turbulent conditions using DNS data, which show an almost linear collapse of the HRR against the rate of the reaction $H + O_2 + M \Leftrightarrow HO_2 + M$, for low and high turbulence levels considered here. Laser diagnostics involving the markers identified in this study would be useful in confirming the proposed correlations. The applicability of these markers for mixtures with various compositions is the subject of future work.

Acknowledgments

ZMN and NS acknowledges the funding through the Low Carbon Energy University Alliance Programme supported by Tsinghua University, China. ZMN also likes to acknowledge the educational grant through the A.G. Leventis Foundation. This work made use of the facilities of HECToR, the UK's national high-performance computing service, which is provided by UoE HPCx Ltd at the University of Edinburgh, Cray Inc. and NAG Ltd., and funded by the Office of Science and Technology through EPSRC's High End Computing Programme. ZMN and NS would also like to thank Y. Minamoto for providing methane–air DNS data.

References

[1] N. Swaminathan, G. Xu, A.P. Dowling, R. Balachandran, J. Fluid Mech. 681 (2011) 80–115.
[2] T.J. Poinsot, A.C. Trouve, D.P. Veynante, S.M. Candel, E.J. Esposito, J. Fluid Mech. 177 (1987) 265–292.
[3] S.M. Candel, Symp. Int. Combust. 24 (1992) 1277–1296.
[4] H.N. Najm, P.H. Paul, C.J. Mueller, P.S. Wyckoff, Combust. Flame 113 (1998) 312–332.

[5] P.H. Paul, H.N. Najm, Symp. Int. Combust. 27 (1998) 43–50.
[6] H.N. Najm, O.M. Knio, P.H. Paul, P.S. Wyckoff, Combust. Sci. Technol. 140 (1998) 369–403.
[7] M.D. Smooke, I.K. Puri, K. Seshadri, Proc. Combust. Inst. 21 (1986) 1783–1792.
[8] A. Gazi, G. Vourliotakis, G. Skevis, M.A. Founti, Combust. Sci. Technol. 185 (2013) 1482–1508.
[9] S. Bockle, J. Kazenwadel, T. Kunzelmann, D.I. Shin, C. Schulz, J. Wolfrum, Proc. Combust. Inst. 28 (2000) 279–286.
[10] C.M. Vagelopoulos, J.H. Frank, Proc. Combust. Inst. 30 (2004) 241–249.
[11] B.O. Ayoola, R. Balachandran, J.H. Frank, E. Mastorakos, C.F. Kaminski, Combust. Flame 144 (2006) 1–16.
[12] A. Fayoux, K. Zhringer, O. Gicquel, J.C. Rolon, Proc. Combust. Inst. 30 (2004) 251–257.
[13] R.L. Gordon, A.R. Masri, E. Mastorakos, Combust. Theory Model. 13 (2009) 645–670.
[14] S.B. Dworkin, A.M. Schaffer, B.C. Connelly, M.B. Long, M.D. Smooke, M.A. Puccio, B. McAndrew, J.H. Miller, Proc. Combust. Inst. 32 (2009) 1311–1318.
[15] B. Ayoola, G. Hartung, C.A. Armitage, J. Hult, R.S. Cant, C.F. Kaminski, Exp. Fluids 46 (2009) 27–41.
[16] M. Roder, T. Dreier, C. Schulz, Appl. Phys. B 107 (2012) 611–617.
[17] K.N. Gabet, R.A. Patton, N. Jiang, W.R. Lempert, J.A. Sutton, Appl. Phys. B 106 (2012) 569–575.
[18] T. Komori, N. Yamagami, H. Hara, Gas Turbine Engineering Section Power Systems Headquarters Mitsubishi Heavy Industries, Ltd. Industrial Report, Design for Blast Furnace Gas Firing Gas Turbine, 2004. <www.mhi.co.jp/power/news/sec1/pdf/2004_nov_04b.pdf>.
[19] Z.M. Nikolaou, N. Swaminathan, Direct Numerical Simulation of multi-component fuel combustion with detailed chemistry, Combust. Flame, October 2013 (submitted for publication).
[20] Y. Minamoto, N. Swaminathan, Combust. Flame 161 (2014) 1063–1075.
[21] Report: Hydrogen from Coal Program: Research, Development, and Demonstration Plan for the period 2008 through 2016. U.S. Department of Energy, 2008.
[22] Report: Wabash River Coal Gasification re-powering Project: A DOE Assesment. U.S. Department of Energy National Energy Technology Laboratory, 2002.
[23] O. Maustard, Report: Massachusetts Institute of Technology Laboratory for Energy and the Environment, An Overview of Coal based Integrated Gasification Combined Cycle (IGCC) Technology, 2005.
[24] R.J. Kee, J.F. Grcar, M.D. Smooke, J.A. Miller, Tech. Rep. SAND85-8240 Sandia National Laboratories, A Fortran Program for Modelling Steady Laminar One-dimensional Premixed Flames, 1985.
[25] R.J. Kee, F.M. Rupley, J.A. Miller, 1992, Chemkin-II: A Fortran Chemical Kinetics Package for the Analysis of Gas Phase Chemical Kinetics, Sandia National Laboratories Report, SAND89-8009B.
[26] G.P. Smith, D.M. Golden, M. Frenklach, N.W. Moriarty, B. Eiteneer, M. Goldenberg, C.T. Bowman, R.K. Hanson, S. Song, W.C. Gardiner, V.V. Lissianski, Z.Qin. <http://www.me.berkeley.edu/gri_mech>.
[27] Z.M. Nikolaou, J.Y. Chen, N. Swaminathan, Combust. Flame 160 (2013) 56–75.
[28] G. Vourliotakis, G. Skevis, M.A. Founti, Energy Fuels 25 (2011) 1950–1963.
[29] Chemical-Kinetic Mechanisms for Combustion Applications, San Diego Mechanism web page, Mechanical and Aerospace Engineering (Combustion Research), University of California at San Diego. <http://combustion.ucsd.edu>.
[30] J. Li, Z. Zhao, A. Kazakov, M. Chaos, F.L. Dryer, J.J. Scire, Int. J. Chem. Kinetics (2006) 109–136.
[31] M.D. Smooke, V. Giovangigli, Formulation of the premixed and non-premixed test problems, in: M.D. Smooke (Ed.), Lecture Notes in Physics, vol. 384, Springer-Verlag, 1991.